Estimation of gas-hydrate concentration and free-gas saturation from log and seismic data

Umberta Tinivella and Jose M. Carcione, Istituto Nazionale di Oceanografia e di Geofisica Sperimentale (OGS), Trieste, Italy

When no direct measurements are available, detailed knowledge of the compressional- and/or shear-wave velocity fields is essential for quantitative estimation of gas hydrate and free gas in bottom-simulating reflectors (BSR). Discrepancies between experimental velocity profiles and the velocity for water-filled sediments reveal the presence of gas hydrate (positive anomalies) and free gas (negative anomalies).

We use the model developed by Carcione and Tinivella (2000), based on a three-phase Biot-type theory, to obtain wave velocities of sediments saturated with water and gas hydrate, and the theory of Santos et al. (1990) to calculate the wave velocities of a porous medium saturated with a mixture of water and free gas. This model assumes that the free gas is uniformly distributed in the pore space. We use a second approach to model patchy saturation of free gas (Dvorkin et al., 1999).

ODP Leg 164, site 995. This site is in the Blake Ridge area offshore South Carolina (Figure 1). Our analysis is focused on borehole 995 because data acquired at sites 994 and 997 were severely affected by enlarging hole conditions. The velocity profile is derived from in situ measurements obtained by VSP.

To obtain the theoretical velocity, we used porosity and density measured in a laboratory. The shear modulus versus depth was obtained by a linear fit of sparse *S*-wave log data. Other parameters, not available from the CDP Leg 164 data set, are obtained from Hamilton's data set for marine sediments (Hamilton, 1979).

Figure 2 compares the theoretical *P*-wave velocity of water-saturated sediments (broken line) and the VSP wave velocity (solid line). The curves indicate that it is possible to estimate the presence of gas hydrate and free gas from the velocity anomaly. As observed by Guerin et al. (1999), compressional- and shear-wave velocity gradients in the gas-hydrate zone are stronger than Hamilton's wave-velocity gradients. This fact can be explained by the consolidation associated with the presence of hydrate.

To obtain the amount of gas hydrate and free gas, we vary their concentrations until we fit the VSP velocity curve. Figure 3 shows the concentrations of gas hydrate and free gas (solid line, positive and negative values, respectively) compared to the corresponding "experimental" values (dots). The broken line represents the theoretical free-gas profile obtained with the patchy-saturation model. The experimental gas-hydrate concentration is obtained from measurements of the chlorinity content. No precise experimental values are available for free gas concentration. The patchy-saturation model predicts more than 10% gas saturation. Nearly 1% was predicted by the three-phase model, for which the gas phase is uniformly distributed in the pore space. Figure 4 shows the difference between the *P*-wave velocities calculated with the patchy-saturation model (broken line) and the uniform-saturation model (solid line) versus free-gas saturation. As can be seen, the decrease in velocity is more pronounced in the second case. Saturation values obtained by Dickens

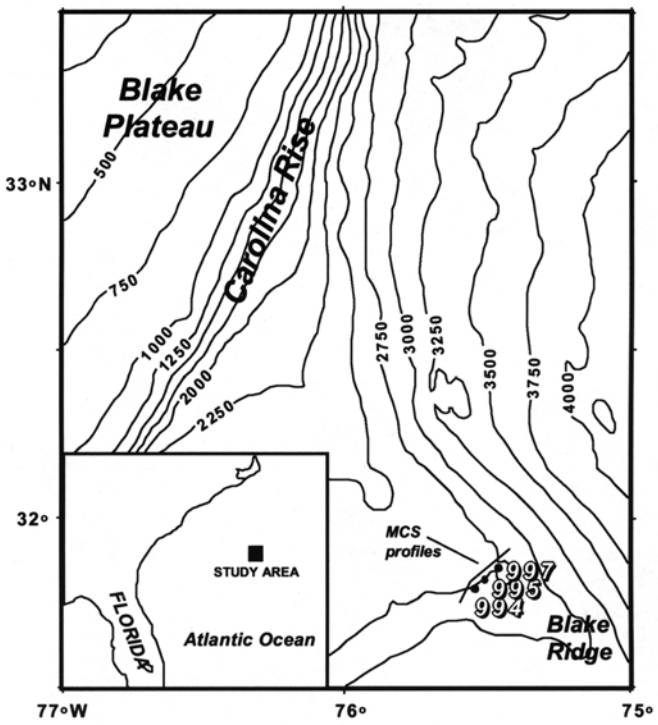

Figure 1. Location of ODP Leg 164, site 995.

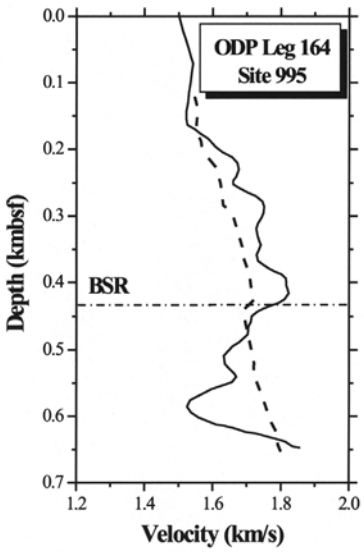

Figure 2. Theoretical *P*-wave velocity of water-saturated sediments (broken line) and VSP wave velocity (solid line) at ODP Leg 164, site 995, Blake Ridge.

(1997)—more than 12%—support the predictions of the patchy-saturation model.

On the other hand, the estimation of gas hydrate is in good agreement with the values obtained from chlorinity data.

ODP Leg 146, site 889. We have also estimated the amount of gas hydrate in the accretionary-wedge sediments of the northern Cascadia subduction zone offshore Vancouver

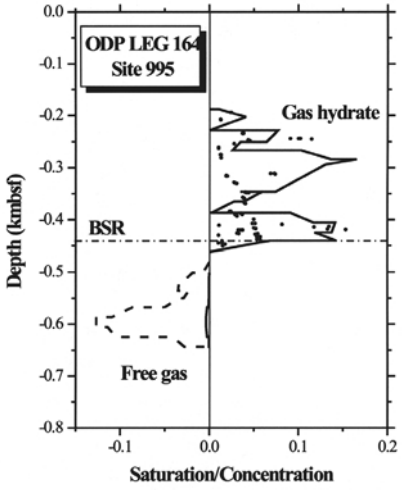

Figure 3. Theoretical concentrations of gas hydrate and free gas (solid line, positive and negative values, respectively) compared to the corresponding experimental values (dots). The broken line represents the theoretical free-gas profile obtained with the patchy-saturation model. The experimental gas-hydrate concentration was obtained from measurements of the chlorinity content (ODP Leg 164, site 995, Blake Ridge).

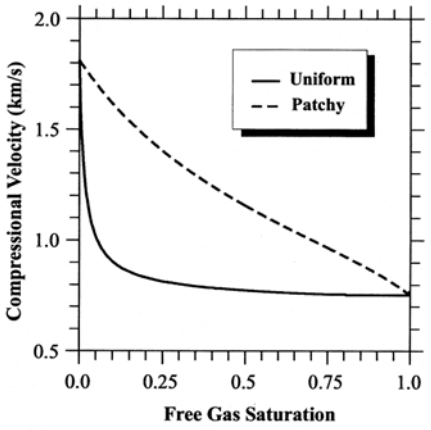

Figure 4. Difference between the *P*-wave velocities calculated with the patchy-saturation model (broken line) and the uniform-saturation model (solid line) versus free-gas saturation.

Island (Figure 5). *P*-wave sonic-log, VSP, and laboratory measurements were used to obtain the theoretical velocities. Because no direct measurement of the shear modulus is available, we assumed a Poisson's ratio of 0.46. This value is supported by the agreement between our reference velocity and the polynomial fit obtained by Yuan et al. (1996) below 120 mbsf (meters below sea floor). We use the reference porosity estimated by Yuan et al.

Figure 6 compares the reference velocity (dotted line) of Yuan et al., the VSP velocity (solid line), and the sonic-log velocity (broken line) at ODP Leg 146, site 889. The reference velocities obtained from the sonic-log and VSP data are close to that of Yuan et al. Note that the decrease in velocity due to free gas is only present in the VSP profile. In the gas-hydrate zone, the anomaly reaches a maximum of 300 m/s at 190 mbsf.

The estimated concentration of gas hydrate is shown in Figure 7. The solid line is the curve obtained from the VSP

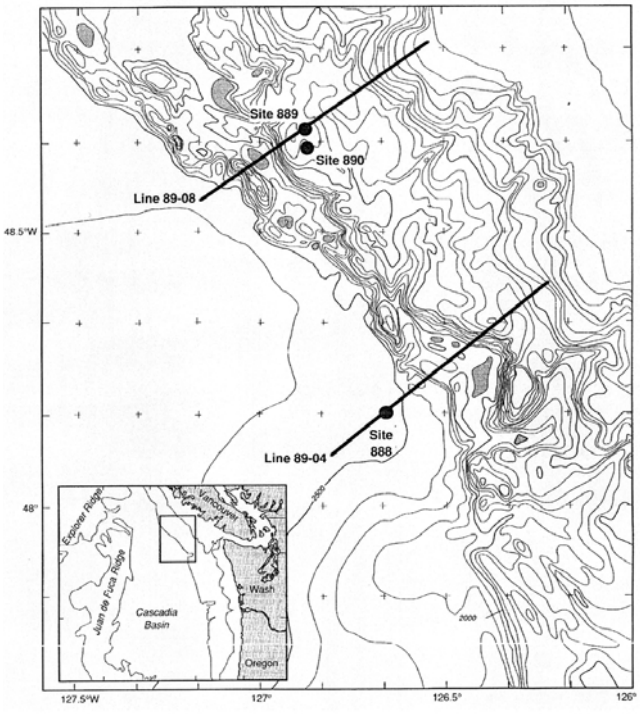

Figure 5. Location of ODP Leg 146, site 889.

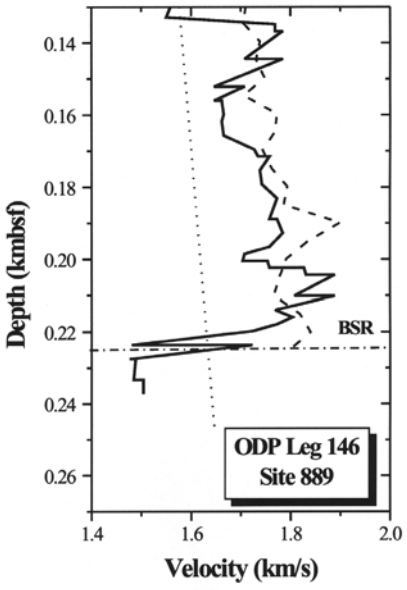

Figure 6. Comparison of the reference velocity of Yuan et al. (dotted line), the VSP velocity (solid line), and the sonic-log velocity (broken line) at ODP Leg 146, site 889.

data, and the broken line is that estimated from the sonic-log data. Triangles and stars indicate concentrations obtained from the chlorinity content and from the time-average equation (Yuan et al., 1996), respectively. Our estimations are closer to the experimental values (triangles) than the values of Yuan et al. On the basis of VSP data, the model predicts free gas below the BSR, even if the chlorine concentration indicates the presence of gas hydrate. The amount of gas saturation predicted by the three-phase model and the patchy-saturation model are approximately 0.25% and 6%, respectively.

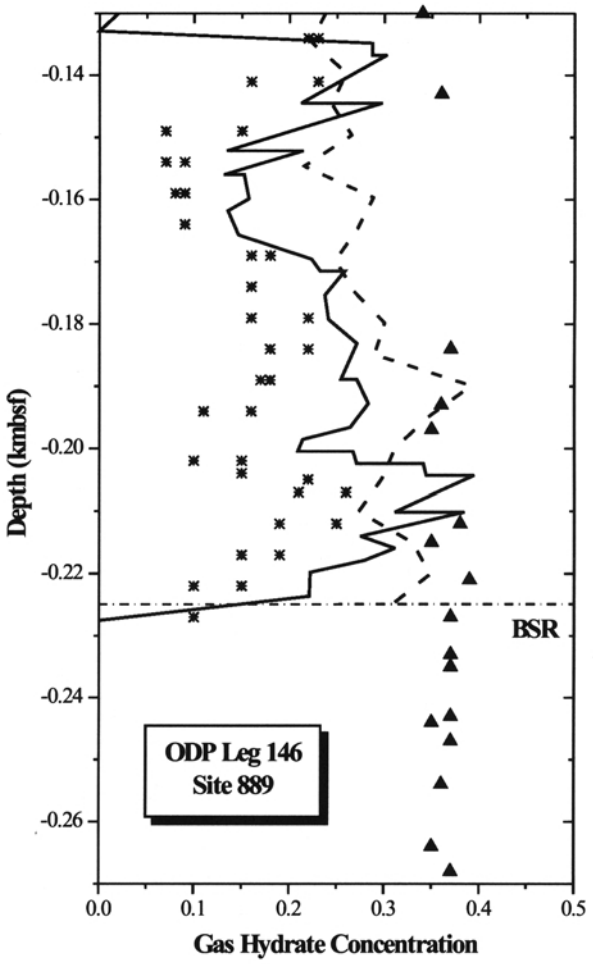

Figure 7. Estimated concentration of gas hydrate at ODP Leg 146, site 889. The solid line is the curve obtained from the VSP data and the broken line is that estimated from the sonic log. Triangles and stars indicate concentrations obtained from the chlorinity content and from the time-average equation of Yuan et al., respectively.

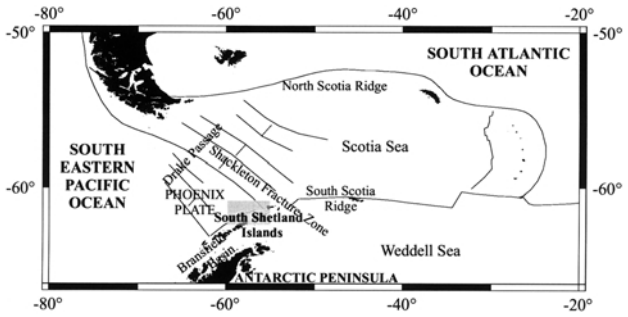

Figure 8. Location of the BSR in the accretionary prism of the South-Shetland Islands (gray rectangle). A set of multichannel seismic lines was acquired in this area by the OGS *Explora* in 1996-97.

South-Shetland Margin of the Antarctic Peninsula. A strong BSR is present in the accretionary prism of the South-Shetland Margin. This strong reflection is caused by the acoustic impedance contrast between gas-hydrate and free-gas saturated sediments. The available data, a set of multichannel seismic lines, were acquired by OGS *Explora* in 1996-97. The area is indicated by a gray rectangle in Figure 8.

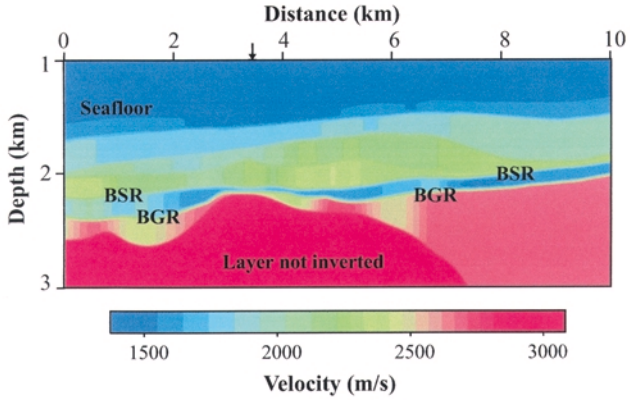

Figure 9. Velocity field across a section parallel to the South-Shetland Margin in Antarctica. The BSR is evident at the left where a low-velocity layer, caused by the presence of free gas, is embedded in a higher velocity background.

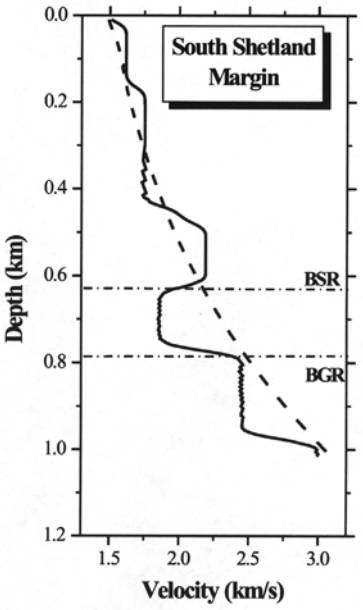

Figure 10. Comparison of the velocity profile at 3500 m (arrow in Figure 9) to the reference velocity profile. Above the BSR, a strong positive velocity anomaly indicates hydrated sediments. The pronounced negative velocity anomaly between the BSR and the BGR (base of the free-gas reflector) reveals the presence of free gas in the sediments.

The velocity field was determined with the commercial software GeoDepth. First, we interpreted the stacked section by picking the main reflectors. On the basis of these picks, the algorithm identified events in the prestack domain using coherence analysis. The velocity analysis provided the initial model for the inversion algorithm. This used ray tracing to compute the moveout curves, and we chose the maximum semblance between data and predictions. This process is performed within a time window around the common midpoints predicted by the ray-tracing algorithm. Next, a depth section was generated using interval velocities obtained with the inversion technique. Finally, the model was refined by a horizon-based global-depth tomography algorithm, using depth delays. These delays give information of the residual error in moveout after prestack migration is applied. This information was used to flatten the gathers. The degree of nonflatness yields a qualitative estimation of the error in the determination of the model. The tomographic algorithm uses these nonflatness estimates and finds an updated model, with minimum error. The input to this process is the above mentioned depth model and the conventional depth model obtained from velocity analysis.

(Continued on p. 203)

(Tinivella, from p. 202)

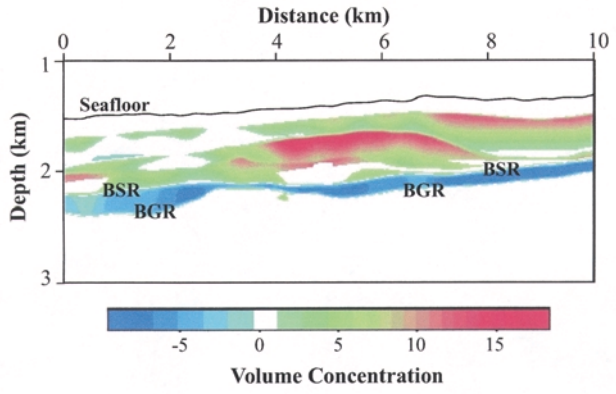

Figure 11. Concentration map of gas hydrate (positive values) and free gas (negative values) corresponding to the BSR offshore the South-Shetland Islands. The figure shows the hydrate concentration (and free-gas saturation) multiplied by the porosity (i.e., the volume concentration). In this way, we can compare the content of hydrate and free gas between zones of different porosity.

In the velocity field (Figure 9), the BSR is evident at the left where a low-velocity layer (≈ 1600 m/s), caused by free gas is embedded in a higher velocity background (≈ 2200 m/s). Figure 10 compares the velocity profile at 3500 m (arrow in Figure 9) to the reference velocity profile. Above the BSR, a strong positive velocity anomaly indicates the presence of hydrated sediments, and the pronounced negative velocity anomaly between the BSR and the BGR (base of free-gas reflector) reveals the presence of free gas. The concentration map is shown in Figure 11, in which velocities of sediments saturated with free gas were obtained with the patchy-saturation model. The figure depicts the hydrate concentration and free-gas saturation multiplied by the porosity (i.e., the volume concentration). In this way, we can compare the content of hydrate and free gas between zones of different porosity. Positive values indicate the presence of gas hydrate and negative values the presence of free gas. The green above the BSR indicates a concentration of hydrate of approximately 5%; the maximum concentration of free gas below the BSR is nearly 8% (blue).

Conclusions. We developed a method to estimate the concentration of gas hydrate and saturation of free gas using log and seismic data. The wave-velocity field is obtained with a three-phase Biot-type theory. We also used a patchy-saturation theory to model the uneven distribution of free gas below the BSR.

In an ideal situation, log data, cores, VSP data, and high-resolution reflection profiles are required. Log and core data are useful to calibrate the rock-acoustics model (density, porosity, dry-rock bulk and shear moduli). VSP data provide a good calibration curve for the velocity field. However, we have shown that even in the absence of complete information, the method provides a reasonable estimation of the concentration of gas hydrate and free gas.

Suggested reading. "Bottom simulating reflectors; seismic velocities and AVO effects" by Carcione and Tinivella (GEOPHYSICS, 2000). "Direct measurements of in situ methane quantities in a large gas-hydrate reservoir" by Dickens et al. (*Nature*, 1997). "Identifying patchy saturation from well logs" by Dvorkin et al. (GEOPHYSICS, 1999). "Characterization of in situ elastic properties of gas hydrate-bearing sediments on the Blake Ridge" by Guerin et al. (*Journal of Geophysical Research*, 1999). "V_P/V_S and Poisson's ratios in marine sediments and rocks" by Hamilton (*Journal of the Acoustical Society of America*, 1979). "Methane hydrate and free gas on the Blake Ridge from vertical seismic profiling" by Holbrook et al. (*Science*, 1996). "A model for wave propagation in a porous medium saturated by a two-phase fluid" by Santos et al. (*Journal of the Acoustical Society of America*, 1990). "Seismic tomography study of a bottom simulating reflector off the South Shetland Islands (Antarctica)" by Tinivella et al. (in *Gas Hydrates: Relevance to World Margin Stability and Climate Change,* Geological Society of London Special Publication 137, 1998). "A method for estimating gas hydrate and free gas concentrations in marine sediments" by Tinivella (*Boll. Geof. Teor. Appl.*, 1999). "Seismic velocity increase and deep-sea gas hydrate concentration above a bottom-simulating reflector on the northen Cascadia continental slope" by Yuan et al. (*Journal of Geophysical Research*, 1996). TLE

Acknowledgments: We are grateful to Zvi Koren and Dan Kosloff of Paradigm Geophysical for providing the GeoDepth software. Discussions with Hans B. Helle of Norsk Hydro are appreciated.

Corresponding author: utinivella@ogs.trieste.it